



Cite this: *Food Funct.*, 2023, **14**, 541

Effect of the simulated digestion process on the chlorogenic acid trapping activity against methylglyoxal

Raffaella Colombo, Mayra Paolillo, Ilaria Frosi, Lucia Ferron and Adele Papetti  *

Chlorogenic acids are hydroxycinnamic derivatives widespread in food or food by-products, known for their antioxidant effects and ability to interfere with the formation of advanced glycation end products (AGEs). AGEs are potential glycotoxins involved in age-related disorders, such as diabetes, cardiovascular diseases, and neurological disorders. The ability of chlorogenic acids to inhibit AGE formation under physiological conditions needs further investigation other than the *in vitro* assays. Therefore, in this study, the capacity of 5-caffeoquinic acid (5-CQA) to effectively trap methylglyoxal (MGO), an AGE precursor compound also present in daily consumed food, was investigated by evaluating 5-CQA and MGO metabolic fate when subjected to digestion. Two different *in vitro* digestion approaches (static based on the Infogest protocol and dynamic based on a novel millifluidic gastrointestinal model) were set up and the samples collected at different steps of the static and dynamic processes were analyzed by a validated RP-HPLC-DAD method. The obtained results indicated that the gastrointestinal process strongly affected the 5-CQA capacity to trap MGO and its resulting antiglycation activity. Therefore, preliminary investigation using advanced *in vitro* tests, particularly dynamic approaches, should always be performed to predict the effect of the digestion process on the potential bioactives present in food, food by-products, or plant extracts.

Received 19th September 2022,
Accepted 11th December 2022

DOI: 10.1039/d2fo02778j
rsc.li/food-function

1. Introduction

Polyphenols are bioactive secondary plant metabolites which have different chemical structures and possess many healthy properties. In fact, a diet rich in polyphenols is believed to promote positive effects, reducing morbidity and the risk of development of many age-related disorders, such as cardiovascular diseases (atherosclerosis and diabetes) and neurodegenerative disorders.^{1–4} In these pathologies, the so-called advanced glycation end-products (AGEs), derived from complex endogenous and exogenous pathways (Maillard or non-enzymatic glycation reaction), play a very important role in toxicity,^{5–7} and the search for molecules that may inhibit AGE effects by different mechanisms has gained importance in the last few years.

Interestingly, fruits, vegetables, and some beverages such as coffee and Cretan tea, together with their food industry by-products, have high contents of bioactive phenolic compounds such as chlorogenic acids and hydroxycinnamic derivatives well known as AGE inhibitors.^{8–14} In the last few years, many

research studies focused on the capacity of caffeoylquinic acids to trap AGE precursors such as α -dicarbonyl compounds. Methylglyoxal (MGO) is one of the most reactive α -oxoaldehyde, and is endogenously formed and also generated in food during processing or storage. It highly contributes to the formation of early Maillard reaction products and AGEs by interacting with aminic groups of arginine and lysine residues and is responsible for damage particularly at the cardiovascular and renal levels.^{15–20}

MGO and also glyoxal (GO)-trapping/inhibitory activity by polyphenols has been generally tested by classical *in vitro* assays, but bioaccessibility and bioavailability studies are mandatory to understand the real efficacy of these bioactive compounds ingested with food. Also, in this case, *in vitro* approaches reproducing gastro-intestinal processes are widely used, and the most common simulated digestion procedures are based on the use of suitable electrolytes and enzyme mixtures mimicking the gastrointestinal tract.^{21–24} To overcome the limitation of such static conventional *in vitro* simulated digestion, we previously set up a new advanced *in vitro* model consisting of modular bioreactors able to simulate flow-mediated transport and absorption of bioactives.²⁵ This model allowed to simulate a dynamic multi-organ passage of MGO under experimental conditions closer to *in vivo* models.

Department of Drug Sciences, University of Pavia, Viale Taramelli 12, 27100 Pavia, Italy. E-mail: adele.papetti@unipv.it; Fax: +39 0382422975; Tel: +39 0382987863



Human gastric stromal cells (GIST-882) and intestinal cancer cells (Caco-2) were selected as cellular models to reproduce a gastro-intestinal system in the simulation of MGO diet intake. By comparing the results obtained in the static (based on an adapted Infogest protocol) and the dynamic *in vitro* procedures, the key role of the gastric compartment in MGO absorption was evident for the dynamic system, differently from that observed using the static assay.

The aim of the present work was to investigate the effect of chlorogenic acid on MGO absorption using the *in vitro* static and dynamic approaches to simulate the gastro-intestinal compartments, in order to better understand the antiglycation properties (specifically MGO trapping capacity) observed for chlorogenic acids.¹¹

2. Experimental

2.1. Reagents and chemicals

LC-grade water and MS-grade water were obtained from a Millipore Direct-QTM system (Merck-Millipore, Milan, Italy). LC- and MS-grade methanol, chloridric acid (37% ACS), perchloric acid (PCA, 70% ACS), calcium chloride dihydrate, potassium dihydrogen phosphate, magnesium chloride hexahydrate ($\geq 99.0\%$), methylglyoxal (MGO, 40% aqueous solution), 3-deoxyglucosone ($\geq 75\%$), *o*-phenylenediamine (OPD, $\geq 98\%$), α -amylase from porcine pancreas type VI-B, pepsin from porcine gastric mucosa (≥ 400 U mg⁻¹), bile extract porcine, pancreatin (8 \times USP) from porcine pancreas protease from *Streptomyces griseus* type XIV (≥ 3.5 U mg⁻¹), viscozyme L cellulolytic enzyme mixture, RPMI-1640 medium, fetal bovine serum (FBS), L-glutamine (200 mM)-penicillin (10 000 U)-streptomycin (10 mg mL⁻¹) solution, poly-L-lysine solution, and the *in vitro* resazurin-based toxicology assay kit were supplied by Merck KGaA (Darmstadt, Germany). 5-O-Caffeoylquinic acid (5-CQA) and 3-O-caffeoylequinic acid (3-CQA) ($>99\%$) were provided by Extrasynthese (Genay, Rhone, France). Acetic acid (96%), sodium chloride, sodium hydroxide pellets, ammonium carbonate, sodium bicarbonate, and potassium chloride were supplied by FarmItalia CARLO ERBA Reagents S.p.A. (Rodano, MI, Italy).

2.2. Standard solution preparation

Standard aqueous solutions of PCA (5 M) and OPD (2.5% w/v), electrolyte solutions for the *in vitro* static simulated digestion process, and hydrochloric acid (6 M) were freshly prepared and stored according to Colombo *et al.*²⁵ and diluted immediately before use. 5-CQA (20 μ M) and 5-CQA (20 μ M)-MGO (80 μ M or 300 μ M) mixtures were prepared by diluting the standard solutions in water or in RPMI-1640 medium added with 10% FBS for the static and dynamic procedures, respectively.

2.3. Cell cultures and cell viability assays

Fondazione IRCCS Istituto Nazionale dei Tumori (Milano, Italy) kindly donated GIST-882 cells, while Caco-2 cells were purchased from the European Collection of Authenticated Cell

Cultures (Salisbury, UK). RPMI medium supplemented with 10% FBS and 200 mM L-glutamine-penicillin (10 000 U)-streptomycin (10 mg mL⁻¹) was used to culture the cell lines, at 37 °C under a controlled atmosphere (5% CO₂-95% air). Confluent cells were split (split ratio 1:5/1:10) by trypsinization and used at the third and fourth passages after thawing. For all the experiments, the cells were plated at a density of 1 \times 10⁴ viable cells per cm².

A resazurin-based assay kit, containing the alamar blue reagent (blue, non-toxic, cell permeable compound and virtually non-fluorescent), which is reduced by viable cells to a highly fluorescent compound, was used to assess cell viability. A 10 \times solution of the reagent was added to the culture medium at 37 °C at the end of the experiments. Samples were collected at different times, and fluorescence was read at 590 nm using an excitation wavelength of 560 nm. Each independent experiment was repeated three times, and each sample was collected in duplicate. The results were expressed as the relative fluorescence intensity (arbitrary units).

2.4. *In vitro* static simulated digestion process

Water solutions of 5-CQA (20 μ M) and of MGO (80 μ M or 300 μ M)-5-CQA (20 μ M) mixtures were prepared and immediately digested. Oral, gastric, and duodenal phases were prepared according to the INFOGEST protocol,²³ while the colon phase was prepared following the procedure of Hamzalioğlu *et al.*²⁸ to simulate a complete gastrointestinal process according to Colombo *et al.*²⁵

2.5. *In vitro* dynamic simulated digestion process

Multi-compartmental modular chambers were set up using the LiveFlow® system (IVTech Srl, Massarosa, LU, Italy) as previously described by Colombo *et al.*²⁵ Briefly, two different chamber configurations were used to simulate the simili-physiological flow through the gastrointestinal digestion process, LB1 (tangential flow) for the gastric compartment (GIST-882 cells) and LB2 (cross-flow - top-down flow) for the intestinal compartment (Caco-2 cells). Gastric and intestinal cells were seeded as previously described and the experimental conditions of the LiveFlow® system were set up (medium volume, flow rate, and connection of chambers).²⁵

After seeding the cells in the sterilized chambers, the LiveFlow® system was placed in a cell culture incubator and the 5-CQA or 5-CQA-MGO mixtures were added to the medium. RPMI medium samples were collected from the system at different time periods (at 4 h from the LB1 chamber; at 1 h, 2 h, 4 h, 6 h, and 24 h from the LB2 chamber). Time 0 (t_0) represented the initial compound concentration before any contact with the cells.

2.6. Sample preparation for 5-CQA and MGO quantification

From each static digestion phase or each monitored time period of the dynamic procedure, two samples were withdrawn and were collected and centrifuged at 5000 rpm for 10 min at 25 °C (Centrifuge 5804 R®, Eppendorf, Mississauga, Ontario, Canada). The supernatants of the 5-CQA and 5-CQA-MGO mix-



tures were incubated with 0.5 M PCA and centrifuged and then derivatized with 0.25% (w/v) OPD at 37 °C for 1 h, according to the protocol of Colombo *et al.*²⁵ Before the HPLC analysis, all the digested samples were filtered (regenerated cellulose (RC) membrane filters, 0.2 µm; Phenomenex®, Torrance, California, USA).

Each independent experiment was repeated three times, and each sample was collected in duplicate.

2.7 RP-HPLC-DAD analysis and method validation

Chromatographic separations of the digested samples were carried out using an Agilent Technologies 1200 series system (Santa Clara, CA, USA). A HPLC system was equipped with a quaternary gradient pump, a manual injector (Rheodyne valve, 20 µL sample loop), a degasser, a thermostatted column oven set at 25.0 ± 0.5 °C, and a diode-array detector (DAD). Data acquisition was performed using ChemStation software (B.04.01) on the Windows XP Professional operating system.

Separations were carried out on a Gemini C-18 column (150 × 2.1 mm, ID; 5 µm; 110 Å) from Phenomenex (Torrance, CA, USA) and a binary mobile phase was used (A: 0.1% formic acid and B: methanol), and a gradient elution of 25 min was performed, which consisted of: 0 to 1 min, 40% B; 1 to 3.5 min, 50% B; 3.5 to 6.5 min, 55% B; 6.5 to 10 min, 70 B %; 10 to 25 min, 40% B. The flow rate was set at 0.3 mL min⁻¹. Chromatograms were recorded at 315 nm (to quantify the signal of 2-methylquinoxaline, which is the MGO quinoxaline derivative) and 325 nm (to quantify 5-CQA and its derivatives).

Specificity, selectivity, linearity, limit of detection (LOD) and limit of quantification (LOQ), accuracy and precision (intra- and inter-day) were evaluated according to the ICH guidelines.²⁹ No peak was observed in the region of the main peaks of MGO and 5-CQA when the chromatographic profiles of RPMI and those of the 5-CQA-MGO mixtures in the medium were compared and therefore the method can be considered specific. No change in the retention time of the analytes in the medium with respect to that of the corresponding standard was observed and therefore the method is also selective. The calibration curves for MGO (5–500 µM) and 5-CQA (5–50 µM) were constructed on the same day and on three consecutive days by plotting the peak area (Y) of the RPMI medium spiked with MGO and 5-CQA at five different experimental concentrations *vs.* the theoretical concentration (X), obtaining a mean correlation higher than 0.9980. LOD and LOQ, defined as the concentration levels at the signal-to-noise ratio of about 3 and 10, were 1.05 µM and 1.5 µM, and 3.25 µM and 5.1 µM, for MGO and 5-CQA, respectively. MGO and 5-CQA recovery values were calculated to determine the method accuracy by analysing three times on three consecutive days, each at three different concentration levels (5–250–500 µM for MGO and 5–25–50 µM for 5-CQA), and the values ranged from 95.06 to 101.98 and 94.98 to 102.34% for MGO and 5-CQA, respectively, indicating that the method is accurate. The same three concentration levels for each analyte were analysed six times within a single day for the intra-day assay and in triplicate per day for three consecutive days for

the inter-day assay, to determine the method precision which was lower than 1.9%.

2.8 Statistical analyses

All data represented the mean ± SD of at least three replicated experiments, each analysed in duplicate. Differences were considered to be significant at *P* ≤ 0.05. All statistical analyses were carried out using Microsoft Excel 2010.

3. Results and discussion

Our previous investigations indicated a high *in vitro* MGO trapping capacity of an aqueous artichoke waste extract rich in chlorogenic acids, among which 5-CQA was present in 20 µM concentration.¹¹ Therefore, the aim of the present work was both to confirm the MGO trapping capacity of this chlorogenic acid isomer and to investigate the effect of the digestion process on such activity. Two different *in vitro* digestion approaches were used to simulate the gastrointestinal digestion. The first one was a slightly modified and integrated INFOGEST protocol, while the second one was a new dynamic simulation model, previously set up by our research group to investigate the metabolic fate of different MGO concentrations, mimicking a meal (80 µM), daily intake (300 µM), and weekly intake (1.3 mM), respectively.²⁵ The metabolic fate of 5-CQA was also investigated to better understand the putative MGO trapping activity under simulated digestion conditions. To monitor the changes occurring during the processes involving the 5-CQA or 5-CQA-MGO mixtures, their concentrations were evaluated by RP-HPLC-DAD after the oral, gastric, duodenal, and colon *in vitro* static digestion steps, and after 4 h in LB1 and after 1, 2, 4, 6 and 24 h in LB2 in the *in vitro* dynamic system. In Fig. 1, a schematic representation of the static digestion approach used in this investigation is shown, while the scheme of the dynamic set up was the same as that was previously reported.²⁵

3.1. 5-CQA trapping capacity against MGO

MGO is a 1,2-dicarbonyl compound promoting the glycation process, and the possibility to trap it by the action of 5-CQA

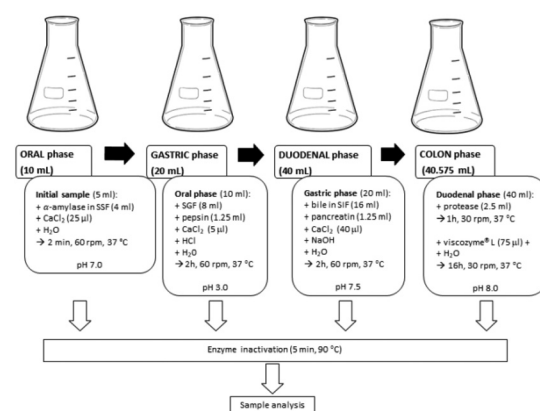


Fig. 1 Flow-chart of the static *in vitro* digestion approach.



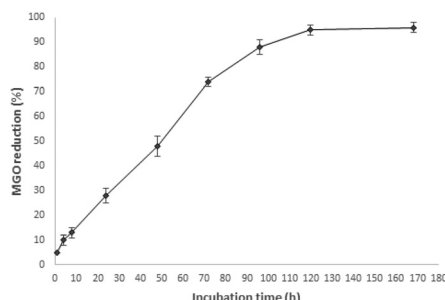


Fig. 2 Kinetic profile of the MGO trapping capacity of the 5-CQA solution (20 μ M).

could represent a good starting point for the identification of natural antiglycation compounds. Considering the activity recorded for an aqueous artichoke waste extract containing 20 μ M 5-CQA, the trapping ability of an aqueous standard solution of 5-CQA at the same concentration was monitored at different time periods in the range of 1 h–7 days (Fig. 2).

The results indicated a good trapping capacity of 5-CQA, starting from 2 days of incubation with increasing activity until five days when 5-CQA was able to quite completely trap MGO. These data confirmed the activities previously reported for chlorogenic acid in coffee silverskin²⁶ and for the isomer 3-CQA tested at about 400 μ M, and show an additional mechanism other than the antiglycation action based on the conjugation with the free amino groups of protein through covalent bonds occurring at 37 °C after 24 h.²⁷

3.2. Effect of the *in vitro* static digestion process at the 5-CQA level

The *in vitro* static approach consisted of four different consecutive simulated digestion phases, *i.e.*, oral, gastric, duodenal, and colon. It is based on the Infogest protocol,²¹ further implemented with the addition of a colon phase according to the procedure of Hamzalioğlu *et al.*²⁸ A 20 μ M 5-CQA aqueous standard solution (subjected to derivatization to compare the results with those obtained by the below reported 5-CQA–MGO mixtures) was digested and the decrease of the 5-CQA concentration after each digestion step was monitored by HPLC and the results are reported in Table 1. The oral and gastric phases did not significantly affect the 5-CQA tested concentration and therefore it seems to be stable even under acidic gastric conditions, as previously generally reported in the literature;^{30–32} conversely, after the duodenal phase 5-CQA level was reduced

Table 1 The 5-CQA concentration (μ M) after each different digestion phase of the static simulated process (n.d., not detected)

Phase	5-CQA (μ M)
Not digested	20
Oral	19.20 \pm 1.30
Gastric	19.37 \pm 1.48
Duodenal	9.35 \pm 0.87
Colon	n.d.

to about 50%, and after the colon phase, no trace of this compound was detected, indicating putative complete 5-CQA metabolism.

The chromatographic profile recorded for each digestion phase is reported in Fig. 3B–E, compared to the undigested mixture (Fig. 3A). The duodenal phase (Fig. 3D) indicated the presence of another peak (R_t : 1.77 min), in addition to that of 5-CQA (R_t : 2.21 \pm 0.01 min), already present in trace in the oral profile (Fig. 3B), identified as 3-O-caffeoylequinic acid (3-CQA) considering its UV-Vis spectrum, selectivity, and co-chromatography with the standard compound.³³ Therefore, the duodenal condition (pH: 7.5 \pm 0.1) highly affected 5-CQA stability, leading to partial isomerization to 3-CQA. Our results are in agreement with those obtained using similar *in vitro* digestion models which have shown that the 3-CQA concentration increased in the duodenal phase because of the acyl-migration under alkaline conditions.³⁴ In addition, other derivatives were detected in the profile of the colon phase (Fig. 3E), which represented 4.1%, 4.1%, and 6.7% of the total peak area, respectively (R_t : 2.88, 4.04, and 4.50 min, respectively). We could speculate that these compounds were generated, following stronger 5-CQA metabolism due to both the incubation for a longer time at 37 °C under basic conditions and being in contact with porcine pancreatin. In fact, Fernandez-Gomez *et al.*³⁵ previously reported the formation of hydroquinone and quinone forms following the incubation of chlorogenic acid at pH 7.4 and 37 °C for 24 h, while Encarnaçao *et al.*³⁶ indicated

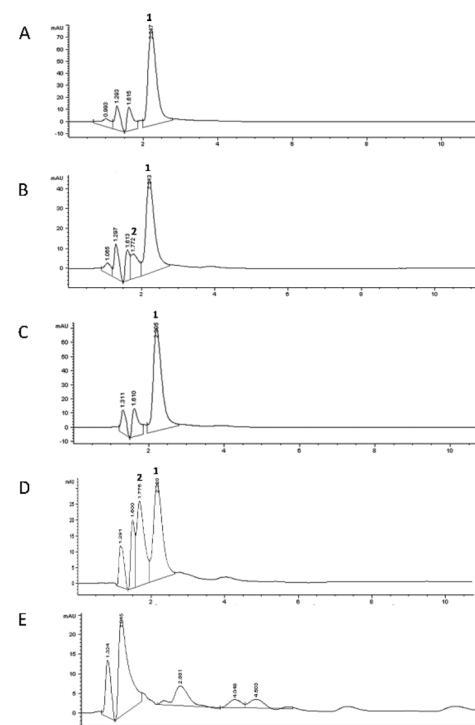


Fig. 3 Chromatographic profiles obtained by RP-HPLC-DAD (325 nm) of the digested sample using the static approach. Undigested 5-CQA solution (A), oral phase (B), gastric phase (C), duodenal phase (D), and colon phase (E). Compound 1, 5-CQA; compound 2, 3-CQA.



5-CQA as a good substrate for pancreatin, a mixture of different enzymes inducing the hydrolysis of this hydroxycinnamic acid derivative to give caffeic acid.

3.3. Effect of the *in vitro* dynamic digestion process at the 5-CQA level

A 20 μM 5-CQA solution was also tested in the dynamic LiveFlow system under the same experimental conditions previously described for MGO:²⁵ 4 h of contact with GIST-882 cells, which is considered a reasonable time frame to simulate a complete gastric digestion³⁷ in the LB1 chamber, and increasing time periods of contact (1, 2, 4, 6, and 24 h) with Caco-2 cells in the LB2 chamber. The results are shown in Table 2.

The 5-CQA concentration in the flowing medium decreased to about 15% after the gastric passage, highlighting a more marked effect than that recorded under static conditions. The HPLC profile recorded for 5-CQA dissolved in the medium before any cell contact (t_0 , Fig. 4A) is characterized by the pres-

ence of another compound eluted at R_t : 3.82 min, observed through the UV-Vis spectrum characterized by two λ_{max} at 265 and 325 nm, respectively. This new species which disappeared after the contact with the GIST cells could be due to the simultaneous influence of the medium and the derivatizing agent, which could promote the formation of a 5-CQA adduct. A more marked reduction in the 5-CQA concentration was recorded after 1 h (Fig. 4C) of contact with the Caco-2 cells (about 20%), and reached to about 60% of the initial concentration after 24 h (Fig. 4D). In this system, partial metabolism of 5-CQA could be speculated. In fact, the HPLC chromatograms recorded for the samples after the contact with Caco-2 cells highlighted the presence of 3-CQA (R_t : 1.75 min, Fig. 4D) and a compound, already generated following the contact with GIST cells (Fig. 4B), characterized by a UV-Vis profile similar to that of 5-CQA and attributable to a hydroxycinnamic acid derivative, of which the concentration increased with increasing contact time with the Caco-2 cells (Fig. 4C and D). The spectral superimposition indicated that this derivative could be the same as that was already detected in the profile of the static colon phase at R_t : 4.04 min (Fig. 3E).

The results obtained using Caco-2 cells differed from those obtained in the colon phase of the static digestion protocol, because in the dynamic system, which better simulates human *in vivo* conditions, 5-CQA is still detectable after 24 h contact without complete metabolism. These data are in agreement with the results obtained by other research groups for this caffeoylquinic acid; 5-CQA is known to be poorly absorbed (by passive diffusion) by Caco-2, independent of the extracellular pH, and to undergo metabolism into caffeic acid.^{32,38} More recently, the presence of an active efflux transport which leads to low intestinal absorption in a Caco-2 cell model was demonstrated.³⁹

In addition, our data are also supported by the results obtained using another dynamic Caco-2 model set up by Scherbl *et al.*⁴⁰ Different from our gastrointestinal model, Scherbl *et al.* only measured the intestinal permeability of chlorogenic acids without considering the gastric step. Also in this case, 5-CQA instability and the isomerization to 3-CQA and 4-CQA were observed. Both studies using two different dynamic systems represent advanced *in vitro* models, which can be considered important approaches to predict the *in vivo* performance of different molecules with potential applications in the food and pharmaceutical fields.

3.4. MGO trapping capacity exerted by 5-CQA under *in vitro* static digestion conditions

In order to evaluate whether 5-CQA could effectively trap MGO under simili-physiological conditions, its effect on two different MGO concentrations (80 μM and 300 μM , mimicking a meal and daily intake, respectively) during the digestion was evaluated using the aforementioned simulated static approach. Two sample solutions containing 20 μM 5-CQA and 80 μM (Mix1) or 20 μM 5-CQA and 300 μM MGO (Mix2) were tested. The concentrations of 5-CQA and MGO after the derivatization procedure using OPD (necessary to give the corresponding

Table 2 The extracellular 5-CQA concentration (μM) at the different monitored time periods after the passage in the multi-compartmental modular bioreactor

Contact time	5-CQA (μM)
0	20
4 h GIST	17.19 \pm 0.85
1 h Caco-2	15.05 \pm 1.09
2 h Caco-2	15.16 \pm 0.72
4 h Caco-2	14.10 \pm 0.71
6 h Caco-2	13.13 \pm 0.66
24 h Caco-2	12.01 \pm 0.48

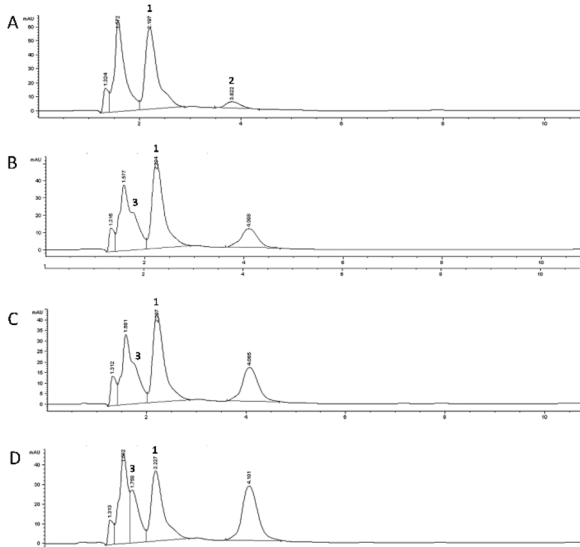


Fig. 4 Chromatographic profiles obtained by RP-HPLC-DAD (325 nm) of the digested sample using the dynamic approach. Undigested sample, t_0 (A), 4 h GIST (B), 1 h Caco-2 (C) and 24 h Caco-2 (D). Compound 1, 5-CQA; compound 2, 5-CQA adduct; compound 3, 3-CQA.



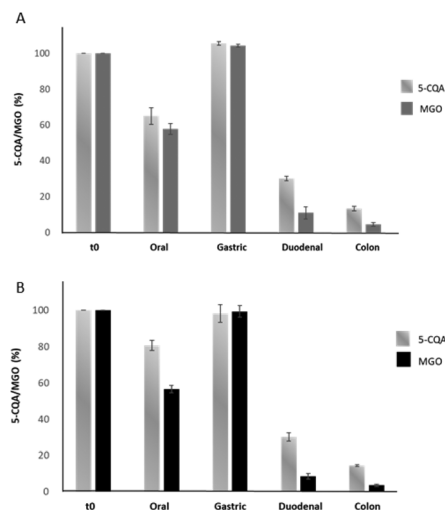


Fig. 5 The detected percentages of 5-CQA and MGO after the oral, gastric, duodenal, and colon steps of the static digestion of Mix1 (20 μ M 5-CQA + 80 μ M MGO) (A) and Mix2 (20 μ M 5-CQA + 300 μ M MGO) (B).

MGO detectable quinoxaline derivative) were monitored at 325 and 315 nm, respectively. In Fig. 5, the results obtained using this approach can be seen.

After the oral step, a reduction of the 5-CQA concentration was recorded for both the mixtures as well as for MGO for which only about 60% of the concentration remained, independent from its starting concentration. The different results obtained for 5-CQA when alone or in mixture with MGO could indicate that 5-CQA alone is not able to form a complex with oral enzymes, different from MGO.²⁵ The gastric phase did not affect 5-CQA and MGO; in fact, their levels were similar to those recorded for the undigested mixtures, indicating that the acidic pH and the presence of pepsin did not promote the metabolism, and therefore the capacity to trap MGO, rather their simple release from a putative complex, originated from the interaction with α -amylase and was promoted by the oral step pH and the contact time between the enzyme and the analytes. Considering the abovementioned findings, the gastric step could be simply considered a phase in which the gastric content is mixed and it can be anticipated that the real digestion step takes place at the duodenal and colon levels.²³ Conversely, a reduction in the MGO and 5-CQA concentrations was recorded after the intestinal phases; in fact, after the duodenal phase only about 30% 5-CQA (about 6.80 μ M) and 10% MGO remained in Mix1 and Mix2 (about 9 and 26 μ M, respectively). These results agreed with the literature data about the effect of basic pH, which promotes the interaction between the analytes and the enzymes (pancreatin) in the *in vitro* static simulated digestion process,²⁸ thereby supporting the metabolism. At the end of digestion (colon step), over 90% 5-CQA and over 95% MGO were metabolized. These results indicated that the metabolism kinetics of 5-CQA was not linked to the MGO concentration, because the recorded profile is very similar to that recorded for the digestion of 5-CQA alone

tested at the same concentration. With regard to MGO, its reduction profile during digestion was independent from its starting concentration in the mixtures and the presence of 5-CQA did not affect its metabolism during the oral and gastric phases, as confirmed by the reduction values similar to those obtained for the digestion of MGO alone tested at the same concentrations.²⁵ Conversely, a more marked reduction, mostly evident at the duodenal level, was recorded for MGO in the mixture with 5-CQA, thus indicating a putative trapping capacity of 5-CQA, previously observed in *in vitro* trapping model systems.¹¹ In any case, MGO in Mix1 and Mix2 was almost totally metabolized at the end of the digestion, as observed when MGO was tested alone.²⁵ The HPLC profile of the colon phase recorded at 325 nm (Fig. 6E) highlighted the presence of a compound at R_t : 4.82 min, of which the spectrum was superimposable with that recorded for the peaks already previously detected at R_t : 4.04 min for 5-CQA, when digested using both the static and dynamic approaches. In addition, another compound at R_t : 3.418 min was better detected at 315 nm only in the colon phase profile of the mixtures, putatively identified as the quinoxaline derivative of 3-deoxyglucosone by comparing the selectivity and UV-Vis spectrum with those obtained after derivatizing the 3-deoxyglucosone standard under the same experimental conditions.

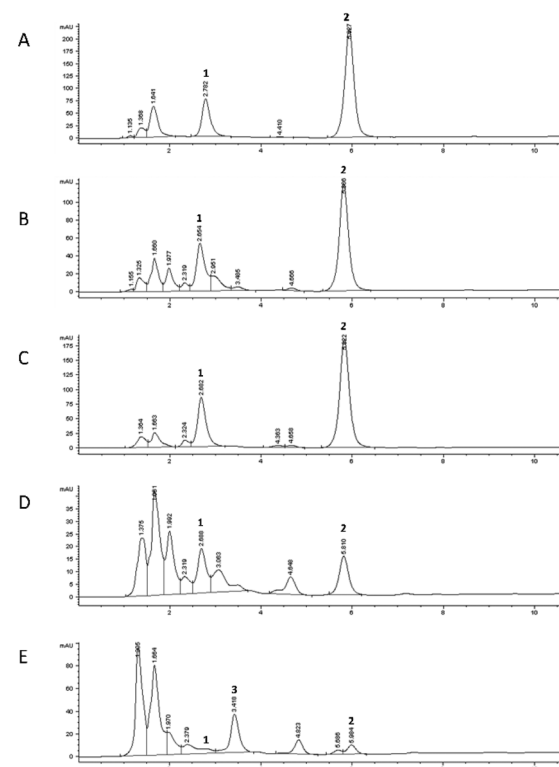


Fig. 6 Chromatographic profiles obtained by RP-HPLC-DAD (325 nm) of the digested sample using the static approach. Undigested 5-CQA solution (A), oral phase (B), gastric phase (C), duodenal phase (D), and colon phase (E). Compound 1, 5-CQA; compound 2, quinoxaline derivative of MGO; compound 3, quinoxaline derivative of 3-deoxyglucosone.

Therefore, 3-deoxyglucosone could be generated by MGO metabolism when MGO is in the presence of 5-CQA.

3.5. MGO trapping capacity exerted by 5-CQA under *in vitro* dynamic digestion conditions

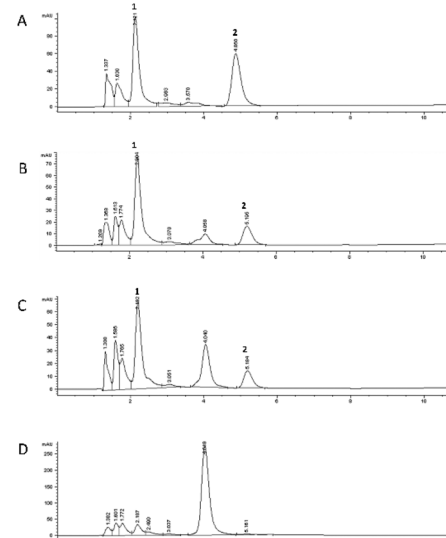
To complete our study on the capacity of 5-CQA to trap MGO during a simulated digestion process, we also tested Mix1 and Mix2 using the dynamic system. The effect of both mixtures on GIST-882 and Caco-2 cell viability was assessed using the alamar blue assay (for more details see Methods section). 20 μ M 5-CQA and 80 and 300 μ M MGO were not toxic on both cell lines when tested alone and in the mixtures during the time period of the digestion process (cell viability was always >95% in the range of 1–24 h).

The 5-CQA and MGO concentrations were monitored after the passage in the GIST-882 and Caco-2 cell compartments, as previously reported for 5-CQA; the concentrations measured at different time periods are shown in Table 3. As it is evident, 5-CQA did not interfere with MGO. In fact, the recorded metabolism trend for 5-CQA and MGO in the mixture was similar to that of every single compound under the same experimental conditions.²⁵ Almost 25% decrease of the 5-CQA concentration was observed after the gastric phase in both mixtures, while after the intestinal passage, a slight decrease until 6 h was observed (35 to 40% of reduction of the initial concentration in Mix1 and Mix2). When the contact time was extended up to 24 h, a significant reduction in the 5-CQA concentration was observed ($p < 0.05$), since only 35% of the initial concentration was detectable in both mixtures. Conversely, only 22–23% of the initial MGO concentration was detected after the gastric phase, independent from the starting concentration, with more rapid kinetics compared to 300 μ M MGO alone.²⁵ After 24 h of contact with Caco-2 cells, MGO was almost no longer detectable both in Mix1 and in Mix2 (lower than 3% of the initial concentration).

Different from the static model, the data from the dynamic system suggested that the gastric phase could represent a key point in the process only when the two compounds are mixed; in fact, during the gastric passage, a decrease of both 5-CQA concentration and MGO concentration was observed, together with the formation of the same 5-CQA compound derivative (R_t : 4.04 \pm 0.01) previously detected in the gastric and intestinal phases of 5-CQA (Fig. 7B–D).

Table 3 The 5-CQA and MGO concentrations (μ M) at the different monitored time periods after the passage in the bioreactor

Contact time	5-CQA (20 μ M) + MGO (80 μ M)		5-CQA (20 μ M) + MGO (300 μ M)	
	20	80	20	300
4 h GIST	14.84 \pm 0.04	17.60 \pm 1.07	15.58 \pm 1.04	68.94 \pm 4.13
1 h Caco-2	13.52 \pm 0.29	13.22 \pm 0.01	14.05 \pm 0.75	52.70 \pm 4.40
2 h Caco-2	13.80 \pm 0.14	11.51 \pm 0.07	13.67 \pm 0.28	46.32 \pm 4.51
4 h Caco-2	13.20 \pm 0.29	8.85 \pm 0.01	12.85 \pm 0.49	35.14 \pm 2.77
6 h Caco-2	12.59 \pm 0.51	7.05 \pm 0.01	12.11 \pm 0.68	27.64 \pm 1.67
24 h Caco-2	7.22 \pm 1.00	2.18 \pm 0.13	6.90 \pm 0.44	8.93 \pm 1.09



Author contributions

Raffaella Colombo: conceptualization, data curation, writing, and original draft preparation. Mayra Paolillo: conceptualization, formal analysis, and data curation. Ilaria Frosi: formal analysis, data curation, and investigation. Lucia Ferron: formal analysis, data curation, and investigation. Adele Papetti: conceptualization, resources, writing – review and editing, and supervision.

Conflicts of interest

There are no conflicts to declare.

Acknowledgements

The authors want to thank the Associazione Italiana Sommelier (AIS), Milan (Italy) delegation and Hotel Siesta, Lido di Camaiore (Italy), for their valuable contributions as financial supporters of the project “Organs in a box: a cure for us, a life for him” (during the years 2018–2020) by Universitiamo, the Pavia University Crowdfunding Platform.

References

- 1 M. Mushtaq and S. M. Wani, Polyphenols and human health: A review, *Int. J. Pharma Bio Sci.*, 2013, **4**, B338–B360.
- 2 G. C. Román, R. E. Jackson, R. Gadhia, A. N. Román and J. Reis, Mediterranean diet: The role of long-chain omega-3 fatty acids in fish; polyphenols in fruits, vegetables, cereals, coffee, tea, cacao and wine; probiotics and vitamins in prevention of stroke, age-related cognitive decline, and Alzheimer disease, *Rev. Neurol.*, 2019, **175**, 724–741.
- 3 I. Arora, M. Sharma, L. Y. Sun and T.O. Tollesbol, The Epigenetic Link between Polyphenols, Aging and Age-Related Diseases, *Genes*, 2020, **11**, 1094.
- 4 P. Ebrahimi and A. Lante, Polyphenols: A comprehensive review of their nutritional properties, *Open Biotechnol. J.*, 2021, **15**, 164–172.
- 5 M. Hellwig, S. Gensberger-Reigl, T. Henle and M. Pischetsrieder, Food-derived 1,2-dicarbonyl compounds and their role in diseases, *Semin. Cancer Biol.*, 2018, **49**, 1–8.
- 6 H. J. Chun, Y. Lee, A. H. Kim and J. Lee, Methylglyoxal causes cell death in neural progenitor cells and impairs adult hippocampal neurogenesis, *Neurotoxic. Res.*, 2016, **29**, 419–431.
- 7 I. Nemet, L. Varga-Defterdarović and Z. Turk, Methylglyoxal in food and living organisms, *Mol. Nutr. Food Res.*, 2006, **50**, 1105–1117.
- 8 A. Gugliucci, D. H. Markowicz Bastos, J. Schulze and M. Ferreira Souza, Caffeic and chlorogenic acids in *Ilex paraguariensis* extracts are the main inhibitors of AGE generation by methylglyoxal in model proteins, *Fitoterapia*, 2009, **80**, 339–344.
- 9 E. Verzelloni, D. Tagliazucchi, D. Del Rio, L. Calani and A. Conte, Antiglycative and antioxidative properties of coffee fractions, *Food Chem.*, 2011, **124**, 1430–1435.
- 10 M. Mesías, M. Navarro, V. Gökmen and F. J. Morales, Antiglycative effect of fruit and vegetable seed extracts: Inhibition of AGE formation and carbonyl-trapping abilities, *J. Sci. Food Agric.*, 2013, **93**, 2037–2044.
- 11 M. Maietta, R. Colombo, R. Lavecchia, M. Sorrenti, A. Zuorro and A. Papetti, Artichoke (*Cynara cardunculus* L. var. *scolymus*) waste as a natural source of carbonyl trapping and antiglycative agents, *Food Res. Int.*, 2017, **100**, 780–790.
- 12 M. Khan, H. Liu, J. Wang and B. Sun, Inhibitory effect of phenolic compounds and plant extracts on the formation of advance glycation end products: A comprehensive review, *Food Res. Int.*, 2020, **130**, 108933.
- 13 I. González, M. A. Morales and A. Rojas, Polyphenols and AGEs/RAGE axis. Trends and challenges, *Food Res. Int.*, 2020, **129**, 108843.
- 14 M. Maietta, R. Colombo, F. Corana and A. Papetti, Cretan tea (*Origanum dictamnus* L.) as a functional beverage: An investigation on antiglycative and carbonyl trapping activities, *Food Funct.*, 2018, **9**, 1545–1556.
- 15 M. Hellwig, S. Gensberger-Reigl, T. Henle and M. Pischetsrieder, Food-derived 1,2-dicarbonyl compounds and their role in diseases, *Semin. Cancer Biol.*, 2018, **49**, 1–8.
- 16 J. Bellier, M. J. Nokin, E. Lardé, P. Karoyan, O. Peulen, V. Castronovo and A. Bellahcène, Methylglyoxal, a potent inducer of AGEs, connects between diabetes and cancer, *Diabetes Res. Clin. Pract.*, 2019, **148**, 200–211.
- 17 R. Kold-Christensen and M. Johannsen, Methylglyoxal Metabolism and Aging-Related Disease: Moving from Correlation toward Causation, *Trends Endocrinol. Metab.*, 2020, **31**, 81–92.
- 18 N. M. J. Hanssen, J. L. J. M. Scheijen, A. Jorsal, H.-H. Parving, L. Tarnow, P. Rossing, C. D. A. Stehouwer and C. G. Schalkwijk, Higher plasma methylglyoxal levels are associated with incident cardiovascular disease in individuals with type 1 diabetes: a 12-year follow-up study, *Diabetes*, 2017, **66**, 2278–2283.
- 19 T. M. Jensen, D. Vistisen, T. Fleming, P. P. Nawroth, P. Rossing, M. E. Jørgensen, T. Lauritzen, A. Sandbæk and D. R. Witte, Methylglyoxal is associated with changes in kidney function among individuals with screen-detected type 2 diabetes mellitus, *Diabetic Med.*, 2016, **33**, 1625–1631.
- 20 N. M. J. Hanssen, C. D. A. Stehouwer and C. G. Schalkwijk, Methylglyoxal stress, the glyoxalase system, and diabetic chronic kidney disease, *Curr. Opin. Nephrol. Hypertens.*, 2019, **28**, 26–33.
- 21 M. Minekus, M. Alminger, P. Alvito, S. Ballance, T. Bohn, C. Bourlieu, F. Carrière, R. Boutrou, M. Corredig, D. Dupont, C. Dufour, L. Egger, M. Golding, S. Karakaya,



B. Kirkhus, S. Le Feunteun, U. Lesmes, A. Macierzanka, A. Mackie, S. Marze, D. J. McClements, O. Ménard, I. Recio, C. N. Santos, R. P. Singh, G. E. Vigarud, M. S. J. Wickham, W. Weitschies and A. Brodkorb, A standardised static in vitro digestion method suitable for food—an international consensus, *Food Funct.*, 2014, **5**, 1113–1124.

22 L. Egger, O. Ménard, C. Delgado-Andrade, P. Alvito, R. Assunção, S. Balance, A. Bradkorb, T. Cattenoz, A. Clemente, I. Comi, D. Dupont, G. Garcia-Llatas, M. J. Legarda, S. Le Feunteun, L. JanssenDuijghuijsen, S. Karakaya, U. Lesmes, A. R. Mackie, C. Martins, A. Meynier, B. Miralles, B. S. Murray, A. Pihlanto, G. Picariello, C. N. Santos, S. Simsek, I. Recio, N. Rigby, L. Rioux, H. Stoffers, A. Tavares, L. Tavares, S. Turgeon, E. K. Ulleberg, G. E. Vigarud, G. Vergères and R. Portmann, The harmonized INFOGEST in vitro digestion method: From knowledge to action, *Food Res. Int.*, 2016, **88**, 217–225.

23 A. Brodkorb, L. Egger, M. Alminger, P. Alvito, R. Assunção, S. Ballance, T. Bohn, C. Bourlieu-Lacanal, R. Boutrou, F. Carrière, A. Clemente, M. Corredig, D. Dupont, C. Dufour, C. Edwards, M. Golding, S. Karakaya, B. Kirkhus, S. Le Feunteun, U. Lesmes, A. Macierzanka, A. R. Mackie, C. Martins, S. Marze, D. J. McClements, O. Ménard, M. Minekus, R. Portmann, N. C. Santos, I. Souchon, R. P. Singh, G. E. Vigarud, M. S. J. Wickham, W. Weitschies and I. Recio, Infocest static in vitro simulation of gastrointestinal food digestion, *Nat. Protoc.*, 2019, **14**, 991–1040.

24 R. Colombo, L. Feron, I. Frosi and A. Papetti, Advances in static in vitro digestion models after the COST action Infogest consensus protocol, *Food Funct.*, 2021, **12**, 7619–7636.

25 R. Colombo, M. Paolillo and A. Papetti, A new millifluidic-based gastrointestinal platform to evaluate the effect of simulated dietary methylglyoxal intakes, *Food Funct.*, 2019, **10**, 4330–4338.

26 M. Rebollo-Hernanz, B. Fernández-Gómez, M. Herrero, Y. Aguilera, M. A. Martín-Cabreja, J. Uribarri and M. D. del Castillo, Inhibition of the Maillard Reaction by Phytochemicals Composing an Aqueous Coffee Silverskin Extract via a Mixed Mechanism of Action, *Foods*, 2019, **8**, 438.

27 B. Fernandez-Gomez, M. Ullate, G. Picariello, P. Ferranti, M. D. Mesa and M. D. del Castillo, New knowledge on the antiglycooxidative mechanism of chlorogenic acid, *Food Funct.*, 2015, **6**, 2081–2090.

28 A. Hamzalioğlu and V. Gökmən, Investigations on the reactions of α -dicarbonyl compounds with amino acids and proteins during in vitro digestion of biscuits, *Food Funct.*, 2016, **6**, 109–114.

29 ICH guideline Q2(R1), *Validation of analytical procedures: text and methodology Guidance for Industry*, 2021.

30 I. D'Antuono, A. Garbella, V. Linsalata, F. Minervini and A. Cardinali, Polyphenols from artichoke heads (*Cynara cardunculus* (L.) subsp. *Scolymus* Hayek): in vitro bioaccessibility, intestinal uptake and bioavailability, *Food Funct.*, 2015, **6**, 1268–1277.

31 H. Yu, H. Jeon, J. Myeong, C. W. Kwon and P.-S. Chang, Influence of creamer addition on chlorogenic acid bioaccessibility and antioxidant activity of instant coffee during in vitro digestion, *LWT-Food Sci. Technol.*, 2021, **151**, 112178.

32 C. Monente, I. A. Ludwing, A. Stalmach, M. P. de Peña, C. and A. Crozier, In vitro studies on the stability in the proximal gastrointestinal tract and bioaccessibility in Caco-2 cells of chlorogenic acids from spent coffee grounds, *Int. J. Food Sci. Nutr.*, 2015, **66**, 657–664.

33 M. N. Clifford, K. L. Johnston, S. Knight and N. Kuhnert, Hierarchical scheme for LC-MSn identification of chlorogenic acids, *J. Agric. Food Chem.*, 2003, **51**, 2900–2911.

34 A. A. Vilas-Boas, A. Oliveira, D. Jesus, C. Rodrigues, C. Figueira, A. Gomes and M. Pintado, Chlorogenic acids composition and the impact of in vitro gastrointestinal digestion on espresso coffee from single-dose capsule, *Food Res. Int.*, 2020, **134**, 109223.

35 B. Fernandez-Gomez, M. Ullate, G. Picariello and P. Ferranti, M.D. Mesa and M.D. del Castillo, New knowledge on the antiglycooxidative mechanism of chlorogenic acid, *Food Funct.*, 2015, **6**, 2081–2090.

36 J. A. Encarnaçao, T. L. Farrell, A. Ryder, N. U. Kraut and G. Williamson, In vitro enzymic hydrolysis of chlorogenic acids in coffee, *Mol. Nutr. Food Res.*, 2015, **59**, 231–239.

37 J. B. Dressman, R. R. Berardi, L. C. Dermentzoglou, T. L. Russell, S. P. Schmaltz, J. Barnett and K. M. Jarvenpaa, Upper gastrointestinal (GI) pH in young, healthy men and women, *Pharm. Res.*, 1996, **7**, 756–761.

38 C. Dupas, A. M. Baglieri, C. Ordonaud, D. Tomé and M. N. Maillard, Chlorogenic acid is poorly absorbed, independently of the food matrix: a Caco-2 cells and rat chronic absorption study, *Mol. Nutr. Food Res.*, 2006, **50**, 1053–1060.

39 O. Mortelé, J. Jörissen, I. Spacova, S. Lebeer, A. L. N. van Nuijs and N. Hermans, Demonstrating the involvement of an active efflux mechanism in the intestinal absorption of chlorogenic acid and quinic acid using a Caco-2 bidirectional permeability assay, *Food Funct.*, 2021, **12**, 417–425.

40 D. Scherbl, S. Muentrich and E. Richling, In vitro absorption studies of chlorogenic acids from coffee using the Using chamber model, *Food Res. Int.*, 2014, **63**, 456–463.

